



# REGIONAL SCALE EARTHQUAKE RISK ESTIMATION BASED ON BROADBAND GROUND MOTION SIMULATIONS

M. Miah<sup>1</sup>, F. Petrone<sup>1</sup>, J. Wong<sup>2</sup>, and D. McCallen<sup>3</sup>

## ABSTRACT

This paper describes a simulation-based framework for assessing regional scale ground motion hazard and resulting structural risk. The exemplifying application presented herein uses two scenarios of broadband (0 to 5 Hz), moderate-to-large magnitude earthquakes. The framework employs two codes: SW4 [1], a parallel 3D finite difference code for characterizing ground motions of high resolution, and NEVADA [2], a nonlinear finite element code for computing inelastic building response of representative steel frame buildings. To achieve realistic ground motion simulations up to 5 Hz, a stochastic representation of geologic heterogeneities is used in the ground motion model. In the building response simulations, structural demands are quantified in terms of peak interstory drift. Approximately 30,000 individual building earthquake response history simulations were executed on a high-performance computing (HPC) platform at the Lawrence Berkeley National Laboratory (LBNL) to provide information on risk variability. A subset of these simulations is summarized and analyzed. The ground motion simulation domains span from near-fault to far-field sites, providing a full breadth of hazard and resulting risk to structures. Correlations of earthquake induced structural demands with various geophysical parameters are explored and some representative distributions of structural demand and damage potential are presented.

---

<sup>1</sup>Postdoctoral Fellow, Earth and Energy Sciences Area, Lawrence Berkeley National Laboratory, 1 Cyclotron Rd., Berkeley, CA 94720 (email: mmiah@lbl.gov, florianapetrone@lbl.gov)

<sup>2</sup>Assistant Professor, School of Engineering, San Francisco State University, 1600 Holloway Ave, San Francisco, CA 94132 (email: jewong@sfsu.edu)

<sup>3</sup>Research Affiliate, Lawrence Berkeley National Laboratory, Associate Vice President, University of California Office of the President, 1111 Broadway, Oakland, CA 94607 (email: david.mccallen@ucop.edu).



## Regional scale earthquake risk estimation based on broadband ground motion simulations

M. Miah<sup>1</sup>, F. Petrone<sup>1</sup>, J. Wong<sup>2</sup>, and D. McCallen<sup>3</sup>

### ABSTRACT

This paper describes a simulation-based framework for assessing regional scale ground motion hazard and resulting structural risk. The exemplifying application presented herein uses two scenarios of broadband (0 to 5 Hz), moderate-to-large magnitude earthquakes. The framework employs two codes: SW4 [1], a parallel 3D finite difference code for characterizing ground motions of high resolution, and NEVADA [2], a nonlinear finite element code for computing inelastic building response of representative steel frame buildings. To achieve realistic ground motion simulations up to 5 Hz, a stochastic representation of geologic heterogeneities is used in the ground motion model. In the building response simulations, structural demands are quantified in terms of peak interstory drift. Approximately 30,000 individual building earthquake response history simulations were executed on a high-performance computing (HPC) platform at the Lawrence Berkeley National Laboratory (LBNL) to provide information on risk variability. A subset of these simulations is summarized and analyzed. The ground motion simulation domains span from near-fault to far-field sites, providing a full breadth of hazard and resulting risk to structures. Correlations of earthquake induced structural demands with various geophysical parameters are explored and some representative distributions of structural demand and damage potential are presented.

### Introduction

Developing a detailed understanding of the regional scale, site-specific variation of earthquake risk to engineered structures is a challenging scientific and engineering problem. Advancements in the quality and distribution of strong ground motion instruments from major earthquakes have provided clearer insight into the complexity of earthquake motions and its implications. This includes the importance of fault rupture mechanics (the source term); complexities of wave

<sup>1</sup>Postdoctoral Fellow, Earth and Energy Sciences Area, Lawrence Berkeley National Laboratory, 1 Cyclotron Rd., Berkeley, CA 94720 (email: mmiah@lbl.gov, florianapetrone@lbl.gov)

<sup>2</sup>Assistant Professor, School of Engineering, San Francisco State University, 1600 Holloway Ave, San Francisco, CA 94132 (email: jewong@sfsu.edu)

<sup>3</sup>Research Affiliate, Lawrence Berkeley National Laboratory, Associate Vice President, University of California Office of the President, 1111 Broadway, Oakland, CA 94607 (email: david.mccallen@ucop.edu).

propagation in a highly heterogeneous geology (path and site response); and the relationship between geophysical parameters and the resulting ground motion frequency content and waveforms (structure-ground motion interaction). However, observational earthquake data is still quite sparse and it remains challenging to gain full understanding into the spatial variation of risk for any specific fault rupture and facility location. In practice, ground motion distribution estimations are based on empirical attenuation relationships that may not be representative of the full richness and complexity of actual variability for a specific fault. Recent advancements in HPC provide a new pathway to gain deeper knowledge on these complex processes, as well as on the implications for optimal, risk-informed seismic design of major infrastructure.

Accurate seismic hazard estimation and corresponding structural risk assessment in both near-fault and far-field regions has been a challenge for scientists and engineers due to the complex spatial variability of ground motions. Traditional strong motion instruments were subject to significant frequency limitations [3] with measured ground records having frequency content limited to waveforms above frequencies of 0.2 Hz ( $T < 5$ s). These records missed important long-period components of motion that can occur in the near-fault region. With the advent of modern digital strong motion instruments, improved measurements of long-period motions are attainable (e.g. period content up to 10s), but the database of observations for near-fault motions is still limited.

Near-fault ground motions are distinguished from far-field ground motions by their strong, low frequency ground displacement and velocity pulses. These low frequency ground motions are associated with fault offset and near-fault wave radiation patterns [4, 5, 6], and can contribute significantly to the risk for longer period structures. By investigating the near-fault ground motion recordings from major earthquakes, Somerville [7] demonstrated that for earthquakes in the range of M6.7 to M7.0, velocity response spectra tend to show peak amplitude for periods between 0.5 and 2.5s. However, for larger events (M7.2 to M7.7), the velocity spectra can exhibit peak response around periods of 4s implicating a potential higher risk for long period structures. Other studies [8] and past observations from earthquakes have shown that early arriving pulses in ground motion time histories can be highly damaging to structures. Anderson and Bertero [9] demonstrated that the duration of a velocity pulse in a ground motion seismogram, in relation to the fundamental period of the structure, is important for determining the degree of nonlinear structural response. In this paper, two simulated broadband (0-5 Hz) earthquake events (M6.5 and M7.0) in a 100 km x 50 km domain are used to characterize structural risk in both near- and far-field regions and assess correlations of structural demands with various geophysical parameters.

### Characteristics of Simulated Near-fault Ground Motions

Figure 1 shows three representative synthetic seismograms and corresponding acceleration and velocity spectra from M6.5 and M7.0 earthquake events based on a massively parallel simulation (7.29 billion grid points) using the finite difference code SW4 [10]. To illustrate the characteristics of near-fault ground motion seismograms, three locations (S1, S2, S3) in the fault vicinity, 4 km adjacent to the fault and along the fault-rupture directivity are inspected in the 100 km x 50 km domain. These sites in the near-fault region are chosen at one-quarter, one-half, and three-quarter distances along the fault to demonstrate how the amplitude of ground motion

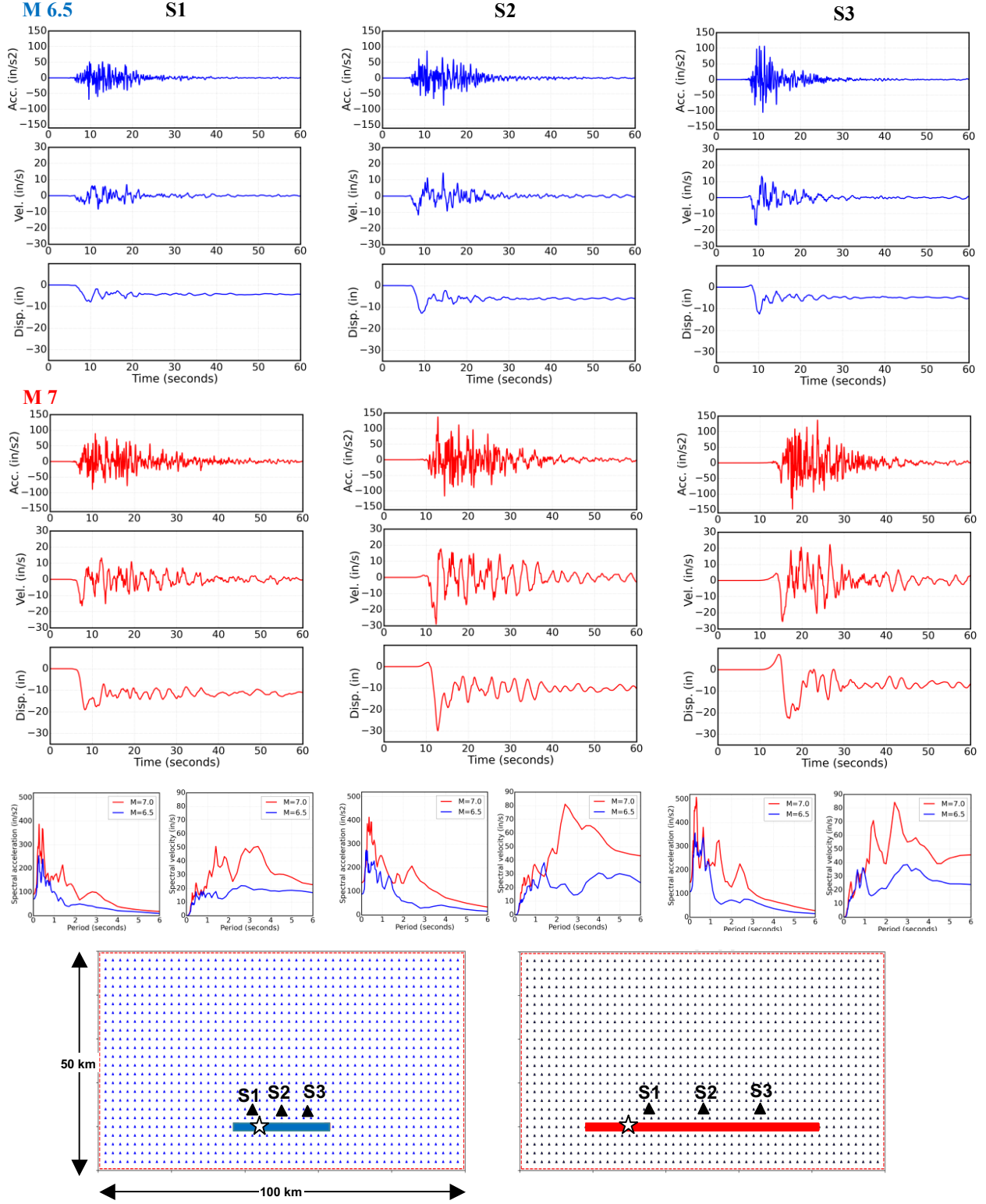


Figure 1. Simulated seismograms, acceleration and velocity spectra for the fault normal (FN) component of ground motion for M6.5 and M7.0 strike slip events at three near-fault locations in a 100 km x 50 km domain. Stars indicate the location of fault rupture initiation for the two events.

varies along the fault and through the fault rupture directivity zone. A detailed description of the fault rupture representation and the characterization of stochastic geology for these simulations is provided by Rodgers et. al. [10], where details about the hypocenter location and rupture propagation along with a discussion on the forward directivity are also discussed. When comparing the ground motion time histories at the three near-field stations for both M6.5 and M7.0 events, the seismogram (S1) closest to the hypocenter exhibits the lowest amplitude for all three parameters (acceleration, velocity, and displacement). Whereas the second (S2) and third (S3) seismograms, both located in the direction of forward rupture directivity and relatively close to the hypocenter, consistently show higher values of ground motion parameters. This is indicative of forward rupture directivity as pointed out by Somerville [7] in his analysis of actual ground motion data for moderate-to-large earthquake events. This forward directivity effect is also reflected in the spectral plots of Figure 1 for the two events, where both velocity and displacement amplitudes increase from station S1 to S3. This increase in spectral amplitude is consistent with results by Abrahamson et. al. in their work comparing NGA ground motions [11].

As an additional observation on the analysis of the synthetic ground motions is that compared to the M6.5 event, the M7.0 event displays a similar peak acceleration magnitude when moving from S1 to S3, but significantly larger pulses in the velocity and displacement histories. In both cases, there is a fault-slip associated permanent ground displacement which increases with event magnitude. For example, considering long periods in the range of 5 to 6 seconds, the M6.5 event shows peak spectral velocity on the order of 18 in/s, 22 in/s, and 24 in/s at stations S1, S2, and S3 respectively, but for the M7.0 event these values are 23 in/s, 43 in/s, and 46 in/s. This significant increase in long-period motions for larger events has the potential to be especially damaging to long-period structures [7], which is manifested in the risk plots shown in Figure 2 and described in the next section.

### Regional Scale Earthquake Risk Characterizations

Two (3- and 40-story) representative steel moment resisting frame (MRF) buildings with representative contributory building mass were employed to analyze nonlinear dynamic response for the two events [2]. Fundamental periods for the 3- and 40-story buildings are 0.91s and 5.5s, respectively. The steel frame building models utilize a finite deformation, inelastic fiber beam element with kinematic hardening [2]. For the discretized 100 km x 50 km domain shown in Figure 1, nonlinear dynamic analyses were conducted by computing the building response for the fault normal (FN) and fault parallel (FP) components of ground motion at selected grid points (station) of the domain in a parallel computation environment. A total of 9,600 nonlinear response history simulations were performed using NEVADA for the two earthquake events. These simulations were executed on the Edison supercomputer at the National Energy Research Scientific Computing Center (NERSC) at LBNL. Figure 2 illustrates regional scale earthquake risk plots for the two events – M6.5 in plots (a) through (d), and M7.0 in plots (e) through (f). The structural risk is defined in terms of the peak interstory drift that occurs in any story of the building over the entire response history. Four risk plots from each event are generated – two for FN and two for FP components of ground motion. The color bar indicates the four interstory drift limits established by the U.S. Department of Energy (DOE) for its facilities [12] and the American Society of Civil Engineers standard for nuclear facilities [13]. Building interstory drift

values from 0% to 0.5% (green) indicate essentially elastic behavior; drift indices from 0.5% to 1% (yellow) indicate limited inelastic response; drifts from 1% to 2.5% (orange) signify moderate inelastic response; and drifts > 2.5% (red) represent significant inelastic response with extensive potential damage to the building.

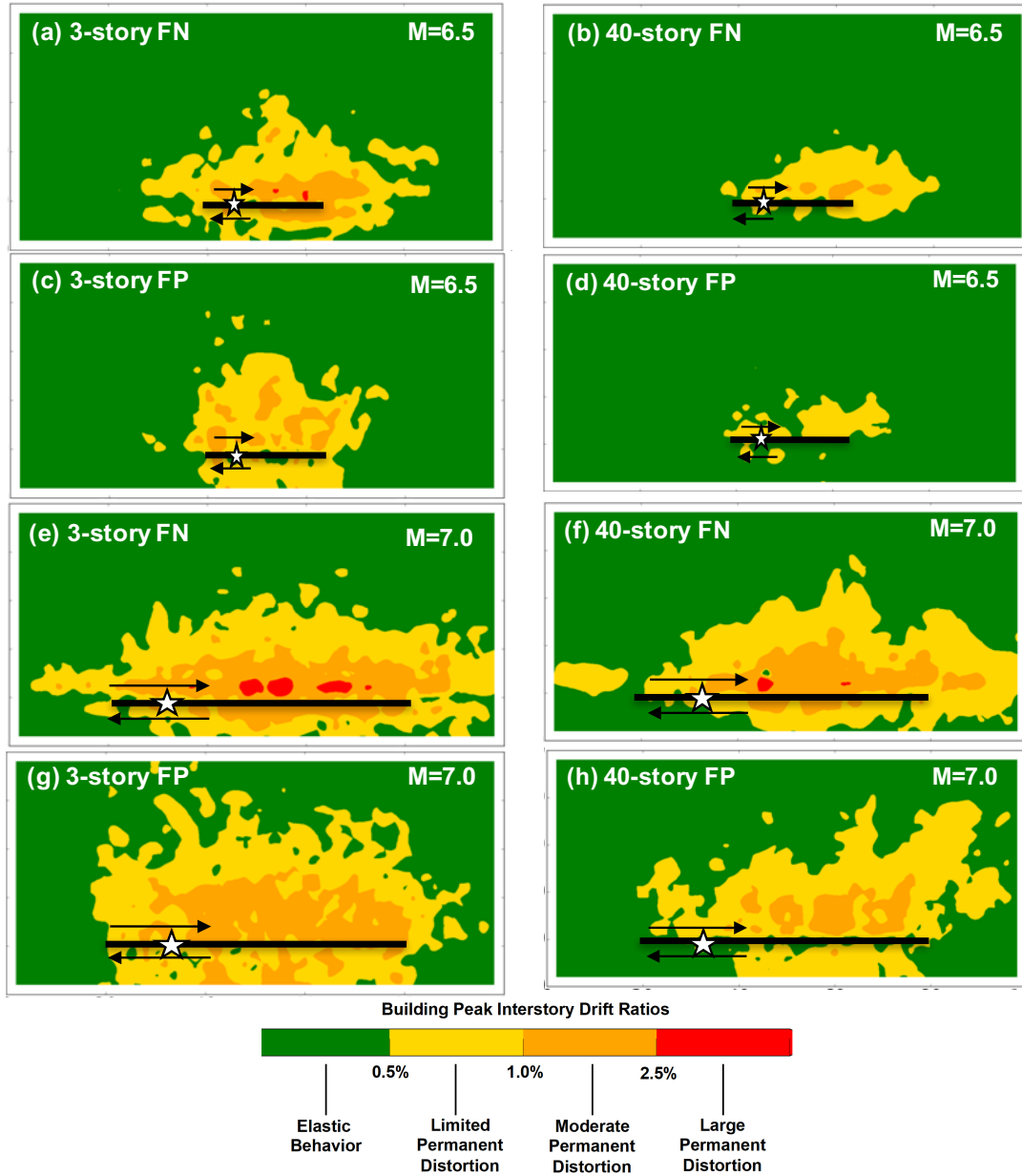


Figure 2. Building peak interstory drift contour plots for 3- and 40-story buildings for M6.5 (a - d) and M7.0 (e - h) events. Color bar and corresponding contours represent the interstory drift limits per ASCE/SEI 43-05.

As expected, the M7.0 event results in a much larger area of risk than the M6.5 event for both buildings. Comparing the building responses from the M6.5 and M7.0 events, the increase in damage potential for the 40-story building is more pronounced due to the increased long-period energy content in the M7.0 event motions (see plot (b), (d), (e), and (f) in Figure 2). The

3-story building does not show such a dramatic increase in damage risk going from M6.5 to M7.0 event as it is not as sensitive to the increased long-period energy.

### Regional Scale Drift Characteristics

To further investigate the relationships between ground motion characteristics and structural risk as predicted by the simulation, fault parallel peak drifts are plotted against fault normal peak drifts for the M7.0 event in Figure 3. Each dot on the plot represents the response of the representative buildings at a specific location in the domain. The color coding of the data points identifies the building's distance from the fault. For example, red dots are the building locations situated within 0 to 10 km (near-fault) of the fault whereas cyan dots represent the buildings located within 30 to 40 km (far-field) away from the fault. A 45-degree diagonal line is drawn to distinguish the individual contribution of risk from the two components of ground motion. Points falling below the line indicate a higher contribution from the FN components and the points lying above the line indicate a higher contribution from the FP component. The data points in the highlighted gray boxes show the FP component tends to contribute more to risk at far-field sites, whereas the FN component tends to contribute the higher risk in the near-fault region, especially for the 40-story building (purple box). This indicates some correlation between simulation model results and what is described by Somerville and Graves in [14] and Somerville in [15] based on the analysis of real records.

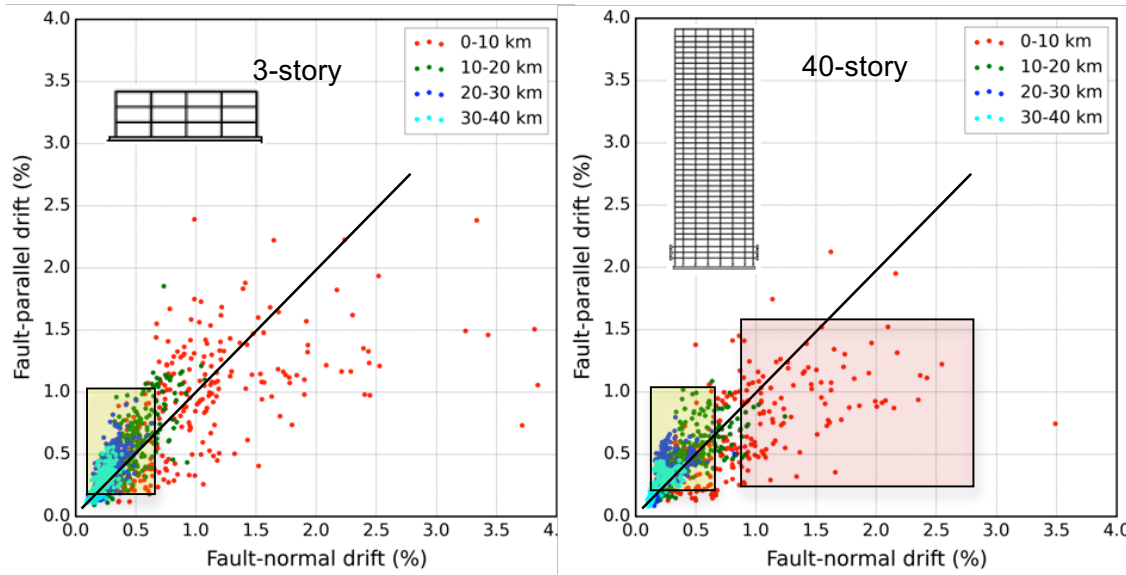


Figure 3. Correlation of fault normal and fault parallel peak interstory drifts for all spatial locations in the computational domain for the M7.0 event.

### Drift Correlations with Spectral Parameters

To gain better understanding of the building response to the simulated earthquake motions, the correlation of building response with spectral parameters was evaluated. For each grid point (station) in the domain, spectral velocity and acceleration were calculated at the fundamental period of the 3-story building and plotted against the peak interstory drift, as shown in Figure 4. Results from a linear-elastic building model (plots a and b) show a very strong correlation

between the spectral parameters (acceleration and velocity) and drift both in near- and far-field, which is indicative of a fundamental mode dominated response. Moreover, a cross comparison with the building response computed using a number of actual near field records from large events (yellow triangles) shows a good agreement with simulated data for both spectral acceleration and velocity.

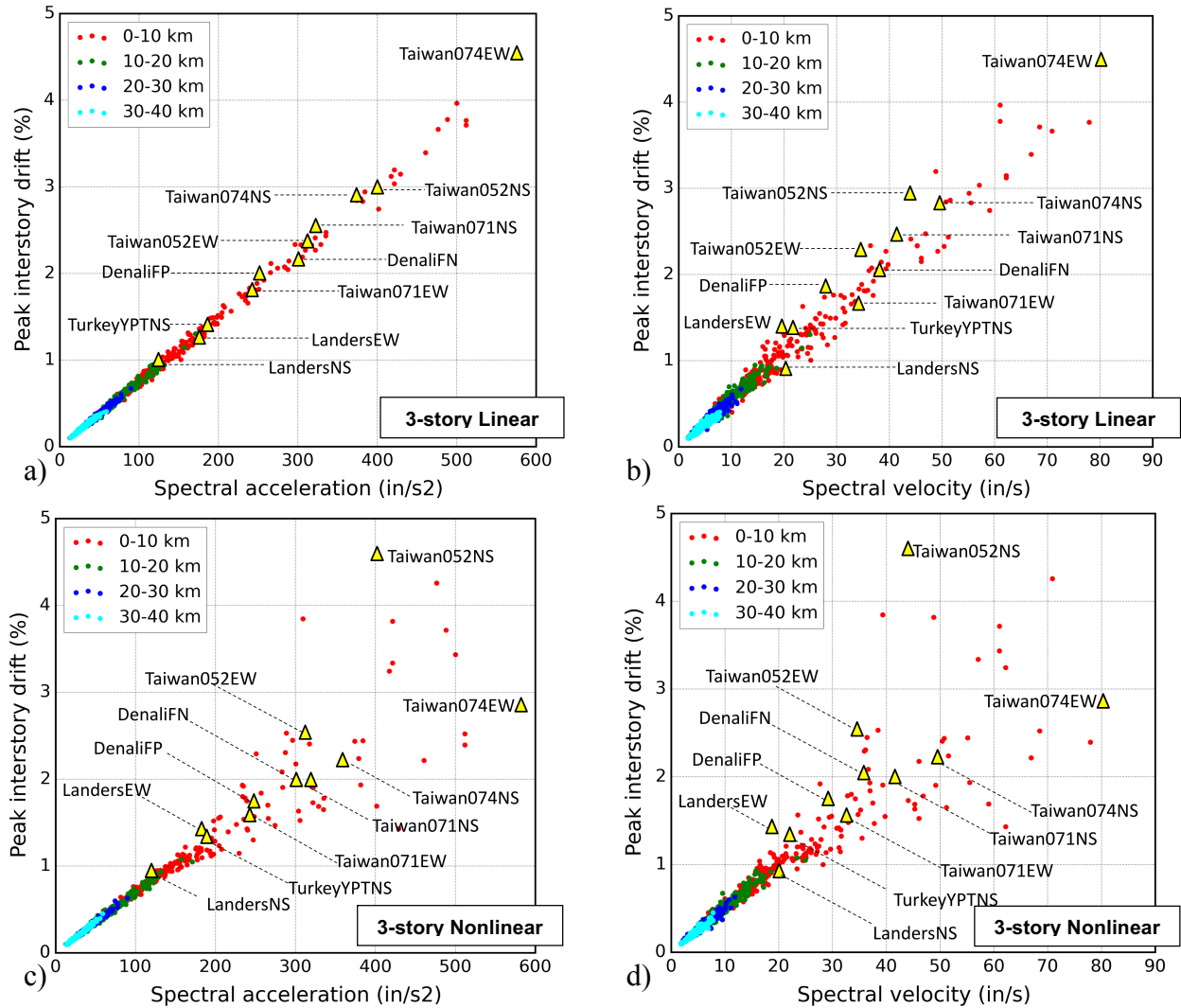


Figure 4. Correlation of peak interstory drift with spectral acceleration (a-c) and spectral velocity (b-d) at period of the fundamental mode of the building for M7.0 event for both linear and nonlinear building models (FN component).

The same comparison for the case of nonlinear building response (plots c and d) indicates a strong linear correlation between peak drift and both spectral parameters in the far-field (>10 km). However, in the near-fault region, where significant inelastic building response occurs, the peak drift is highly variable with very little correlation. Consistently with what is observed in the linear case, the building response from the synthetic ground motion records shows a very similar trend as the building response obtained from response history simulations with actual ground motion records, which lends support to the realism of the synthetic motions in representing

ground motions characteristics. For both synthetic and real motions, the complex distribution of structural risk in the near-fault region for nonlinear models poses a challenge for design engineers. Overall further study and evaluation is necessary to provide increased insight and improved design guidelines especially for structures built in the near-fault region. Similar plots for the 40-story building are shown in Figure 5. For the taller building the correlation of peak drift with spectral acceleration is evident but it is not nearly as strong as for the 3-story building (comparing Figures 5a and 4a). This is indicative of higher mode contributions to the overall taller building response. In addition, the building response with actual records shows more scatter in peak building response, even for the linear building analyses.

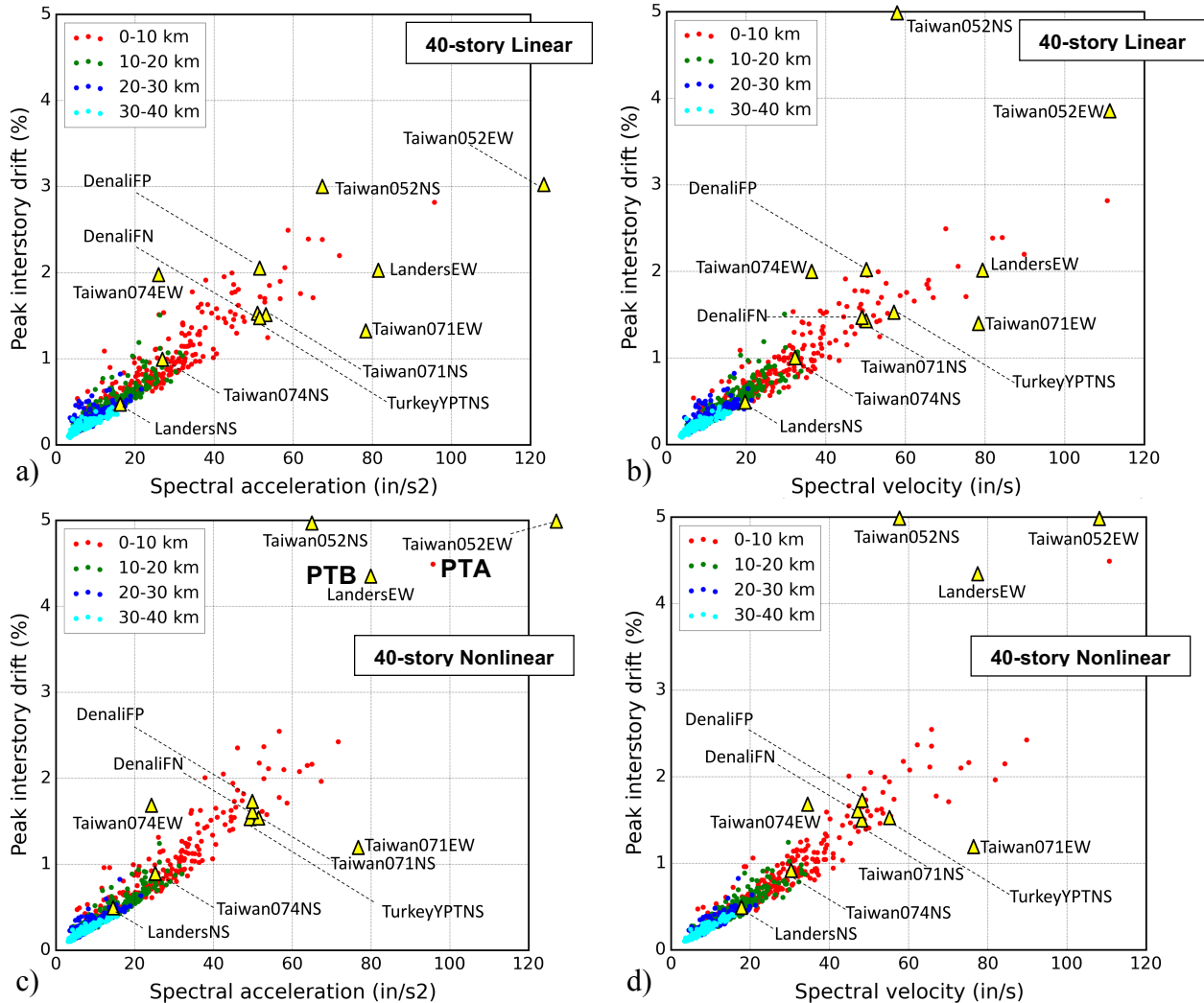


Figure 5. Correlation of peak interstory drift with spectral acceleration (a-c) and spectral velocity (b-d) at period of the fundamental mode of the building for M7.0 event for both linear and nonlinear models (FN component).

For the nonlinear analyses of the 40-story building there are a small number of synthetic and real records that result in extreme drifts in the building (plots c and d). Inspection of the 40-story nonlinear building response from the synthetic records indicates significant sensitivity to the waveforms of long period motions. Figure 6 for example shows the peak interstory drift

envelopes for the 40-story building at two sites located 2 km off the fault and 2 km apart (site locations shown inset on the computational domain). The building response at one site exhibits much larger drifts than the other site as a result of a stronger velocity and displacement pulse. In addition, comparing the interstory drift envelope from a simulated site (located at the orange triangle in the domain) with large drifts from the LandersEW near field motion (inset red drift profile in Figure 6) shows a very similar drift profile from the synthetic and real records (the corresponding points for the peak building response for these synthetic and real records are indicated as “PT A” and “PT B” in Figure 5c).

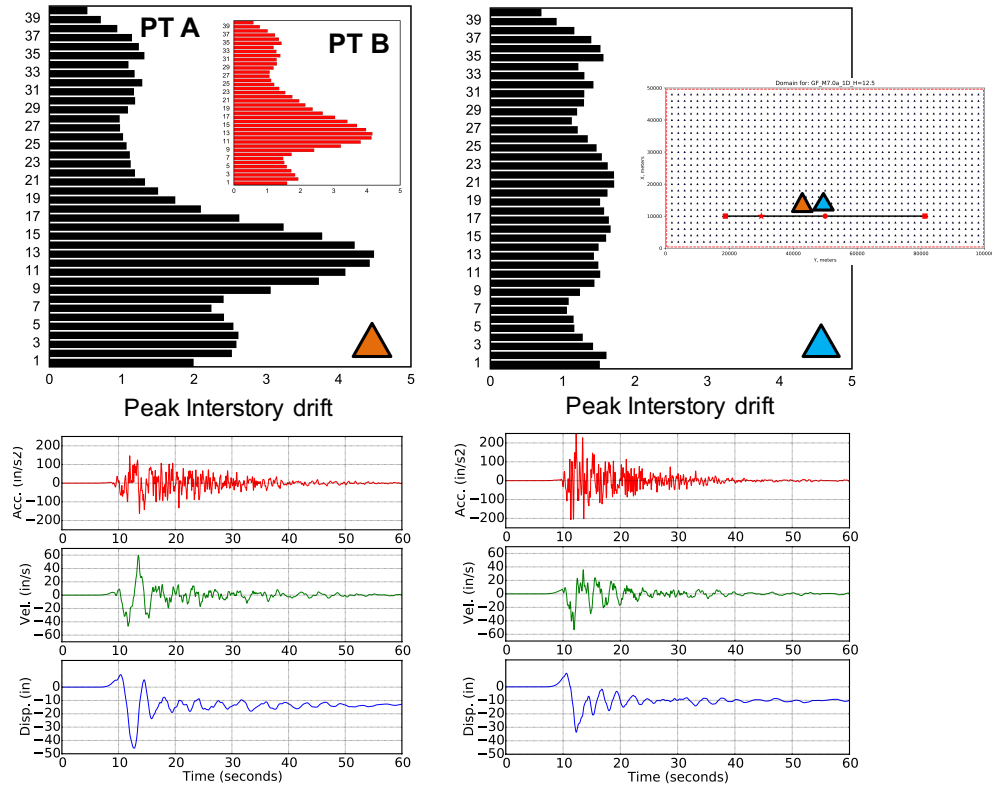


Figure 6. Comparison of 40-story building peak response envelope for two simulated motions from nearby sites (locations on computational domain in inset), “PT A” and “PT B” reference locations indicated in Figure 5c.

### Conclusions

In this paper full-broadband (0-5 Hz) simulated ground motion data were employed to quantify seismic risk for representative building structures on a regional scale. A total of 9,600 nonlinear structural dynamic simulations were performed and analyzed to study the risk variation on a 100 km x 50 km domain for two events (M6.5 and M7). Confirming observations from several literature works, results show there is higher risk for buildings in the proximity of the fault rupture and in the fault-rupture directivity zone. Results also show that, in terms of the influence of motion components considered in analysis, the FN components of motion produce higher drifts in the near-fault region especially for the tall building whereas FP components produce higher drifts in the far-field for both short and tall buildings. Drift correlations with spectral acceleration and spectral velocity demonstrate a strong relation in the far-field. However, in the near-fault region, there is a poor correlation between peak drift and spectral acceleration for

buildings exhibiting nonlinear response. Comparison of these trends with building response from actual near-fault records shows very similar trends for both the linear and nonlinear response cases, which is seen as an indication of the realism of the synthetic ground motions employed in the proposed simulation-based framework for risk estimation. Much work needs to be done to validate the realism of end-to-end, high-performance simulations that span all the way from fault rupture to structural response, but the early results from work underway are very encouraging.

### Acknowledgments

This research was supported by the Exascale Computing Project (ECP), Project Number: 17-SC-20-SC, a collaborative effort of two DOE organizations -- the Office of Science and the National Nuclear Security Administration.

### References

1. Sjogreen B, Petersson NA. A fourth order accurate finite difference method for the elastic wave equation in second order formulation. *J. Sci. Comput.* 2012; **52**(1):17-48. DOI: 10.1007/s10915-011-9531.
2. McCallen D, Larsen S. NEVADA- A simulation environment for regional estimation of ground motion and structural response. A final report submitted to the U.S. DOE by the Lawrence Livermore National Laboratory Directed Research and Development, Project #02-ERD-044, 2003.
3. Trifunac MD, Udwadia FE, Brady AG. Analysis of errors in digital strong-motion accelerograms. *Bull Seismol Soc Am* 1973; **63**:157-87.
4. Bouchon M. The motion of the ground during an earthquake: 1. The case of a strike slip fault. *J. Geophys. Res.* 1980; **85**:356–366.
5. Somerville PG, Smith NF, Smith R, Graves W, Abrahamson NA. Modification of empirical strong ground motion attenuation relations to include the amplitude and duration effects of rupture directivity. *Seism. Res. Lett.* 1997; **68**(1): 199–222.
6. Dreger D, Hurtado G, Chopra A, Larsen S. Near-fault across-fault seismic ground motions. *Bull Seismol Soc Am* 2011; **101**:2.
7. Somerville PG. Magnitude scaling of the near fault rupture directivity pulse. *Phys. Earth Planet. Interiors* 2003; **137**(1):12.
8. Bertero V, Mahin S, Herrera R. Aseismic design implications of near-fault San Fernando earthquake records. *Earthquake Eng. Struct. Dyn* 1978; **6**(1):31–42.
9. Anderson JC, Bertero VV. Uncertainties in establishing design earthquakes. *J. Struct. Eng.* 1987; **113**(8):1709–1724.
10. Rodgers A, Petersson NA, Pitarka A, Miah M, McCallen D, Jeremic B. HPC Simulations of Broadband Near-Fault Ground Motions for Engineering Applications. *Proceedings of the 11th National Conference on Earthquake Engineering*. Earthquake Engineering Research Institute: Los Angeles, 2018.
11. Abrahamson N, Atkinson G, Boore D, Bozorgnia Y, Cambell K, Chiou B, Idriss IM, Silva W, Youngs R. Comparisons of the NGA Ground-Motion Relations. *Earthquake Spectra* 2008; **24**:45-66.
12. DOE. *Natural Phenomena Hazards Design and Evaluation Criteria for Department of Energy Facilities*. U.S. Department of Energy STD-1020-2002. 2002.
13. American Society of Civil Engineers (ASCE). *Seismic Design Criteria for Structures, Systems, and Components in Nuclear Facilities*. ASCE/SEI 43-05. 2005.
14. Somerville, P.G., and Graves, R., Conditions that give rise to unusually large long period ground motions, *The structural design of tall buildings*, 1993, Vol. 2, pp. 211-232.
15. Somerville, P.G., Engineering characterization of near fault ground motions, Proceedings of 2005 NZSEE Conference, Taupo, New Zealand, 2005.